

The Open University's repository of research publications
and other research outputs

Theoretical study of resonance formation in microhydrated molecules. I. Pyridine-(H₂O)_n, n = 1,2,3,5

Journal Item

How to cite:

Sieradzka, Agnieszka and Gorfinkiel, Jimena D. (2017). Theoretical study of resonance formation in microhydrated molecules. I. Pyridine-(H₂O)_n, n = 1,2,3,5. *Journal of Chemical Physics*, 147(3), article no. 034302.

For guidance on citations see [FAQs](#).

© 2017 The Authors

Version: Accepted Manuscript

Link(s) to article on publisher's website:
<http://dx.doi.org/doi:10.1063/1.4993941>

Copyright and Moral Rights for the articles on this site are retained by the individual authors and/or other copyright owners. For more information on Open Research Online's data [policy](#) on reuse of materials please consult the policies page.

**Theoretical study of resonance formation in microhydrated molecules (I):
pyridine-(H₂O)_n, n=1,2,3,5**Agnieszka Sieradzka¹ and Jimena D. Gorfinkiel¹*School of Physical Sciences, The Open University, Walton Hall, Milton Keynes,
MK7 6AA, United Kingdom*

(Dated: 30 June 2017)

We present R-matrix calculations for electron scattering from microhydrated pyridine. We studied the pyridine-H₂O cluster at static-exchange (SE), SE + polarization and close-coupling levels and pyridine-(H₂O)_n n=2, 3 and 5 at SE level only in order to investigate the effect of hydrogen bonding on the resonances of pyridine. We analyse the results in terms of direct and indirect effects. We observe that the total (direct plus indirect) effect of microhydration leads to the stabilization of all resonances studied, both shape and core-excited. The size of this shift is different for different resonances and seems to be linked to the dipole moment of the cluster.

PACS numbers: Valid PACS appear here

Keywords: electron scattering, resonances, microhydration

INTRODUCTION

Electron scattering from polyatomic and, in particular, biological molecules has been studied experimentally and theoretically for at least a couple of decades¹. This research has tended to focus on gas phase/isolated molecules, fundamentally because the techniques and methods required to obtain and interpret results are simpler and more established. The study of these collisions was given significant impulse by the confirmation² that low energy electrons produced when radiation is incident on biological matter can damage DNA via dissociative electron attachment (DEA). Significant effort was placed into the study of electron scattering from DNA components, particularly nucleobases both experimentally (the focus being on studying DEA by mass spectroscopy) and, later on, computationally (where a lot of emphasis has been placed on the investigation of the temporary negative ions, or resonances, that lead to DEA). The work has more recently been extended to other types of biomolecules, in particular aminoacids³.

Concurrent to the study of DNA constituents, targets that can be described as 'model' molecules have been investigated³. These are, for example, tetrahydrofuran, which may be regarded as the elementary prototype of deoxyribose, and pyrimidine, the diazine from which the pyrimidinic nucleobases derive. These systems have been chosen because studying them is easier than treating the relevant biomolecule: this is particularly the case for calculations, where fewer electrons and higher symmetry reduce the computational resources required. All these studies have provided much insight into the collision process. However, biological radiation damage occurs in a condensed environment where all molecules with a biological function are surrounded by other molecules, mainly water.

Hydrated clusters have been proposed as systems that bridge the gap between the pure gas phase and the actual environment in which radiation damage takes place. From a theoretical point of view, microhydrated systems are more electron rich, but can be treated using the same methodology as isolated molecules. Studies⁴ of CH₂O-H₂O and singly and doubly hydrated formic acid⁵ and phenol⁶ using the Schwinger Multichannel Method have been performed. These showed that, at Static-Exchange (SE) level, water acting as hydrogen donor 'stabilizes' (lowers the energy of) the resonances but when it acts as the hydrogen acceptor, the resonances are 'destabilized' (i.e. the resonance shifts to higher energies). Static-exchange plus Polarization (SEP) calculations were also performed for these systems,

According to the same qualitative results. We note that it is not always clear in these papers what geometry has been chosen to perform calculations for the isolated molecule in order to compare the resonance positions and that this, as we show later, may have a bigger effect than expected. A couple of experiments^{7,8} have been performed under conditions that ensure only a few water molecules are hydrogen-bonded to the biomolecule. These experiments show quenching of some of the DEA channels, but this is ascribed by the authors to nuclei-related caging effects rather than changes to resonance spectrum and characteristics. Finally, the cross section for dehydrogenation from uracil/thymine has been calculated⁹ (similar work was performed for clusters¹⁰ of CF_2Cl_2 or CF_3Cl and 3 or 6 water molecules); the results of these work will be discussed in Paper II¹¹.

In this paper, we present results from a study of clusters of a single pyridine molecule (the singly substituted benzene ring C_5NH_5) and water. Resonances in isolated pyridine (Pyr) have been studied both using the R-matrix¹² (shape and core-excited) and Schwinger Multichannel¹³ methods (shape only). The properties that influence electron scattering are very similar in this molecule and pyrimidine and so is their resonance spectrum. However, current experiments point at different DEA processes. Pyridine provides a single point (the nitrogen atom) for a hydrogen bond in which it is the acceptor. This means that, as more water molecules are added to the cluster, these form hydrogen bonds among themselves. This is a completely different behaviour to thymine (see Paper II) where the water molecules attach to different (oxygen and hydrogen) atoms in the pyrimidinic ring. Therefore these two systems allow us to investigate a somewhat different effect of adding water molecules to a cluster.

Our aim is to investigate how the resonances present in pyridine are affected by microhydration. Comparison with isolated pyridine allow us to investigate in detail the effect that hydration has on shape and core-excited resonances. In the companion paper (Paper II), we apply the knowledge gained investigating pyridine and we compare these results with those for thymine-water clusters.

II. R-MATRIX METHOD

The R-matrix method is one of several methods used to solve electron-molecule scattering problems within the fixed-nuclei approximation. Its basis is the division of configuration

is divided into two regions: inner and outer. The boundary between these regions is defined by an R-matrix sphere of radius a . In the inner region, the problem is a many-body one and the scattering electron becomes indistinguishable from the electrons of the target. Both exchange and correlation effects must be taken into account. This makes the inner region calculation complex and computationally demanding.

In the inner region, the eigenfunctions of the total (electronic) Hamiltonian for the system, \mathcal{H} , for each irreducible representation denoted by Γ are expanded in the following way:

$$\Psi_k^\Gamma(\mathbf{x}_1, \dots, \mathbf{x}_{N+1}) = \mathcal{A} \sum_{i=1}^{n_b} \sum_{j=1}^{n_b} \Phi_i(\mathbf{x}_1, \dots, \mathbf{x}_N) \gamma_{ij}(\mathbf{x}_{N+1}) a_{ijk} + \sum_{i=1}^m \chi_i^\Gamma(\mathbf{x}_1, \dots, \mathbf{x}_{N+1}) b_{ik}, \quad (1)$$

where \mathcal{A} guarantees the antisymmetrization of the whole wave function. The functions $\Phi_i(\mathbf{x}_1, \dots, \mathbf{x}_N)$ describe bound electronic states of the molecular/cluster target; the number of states included is indicated by n_b . The functions $\gamma_{ij}(\mathbf{x}_{N+1})$ describe the unbound (scattering) electron and are the only single-particle functions which do not vanish on the surface of R-matrix sphere. The last set of functions, $\chi_i^\Gamma(\mathbf{x}_1, \dots, \mathbf{x}_{N+1})$, are L^2 integrable functions that describe the short-range correlation polarization effects. A good description of polarization is essential to obtain accurate resonance parameters as well as accurate low energy cross sections. The density associated to these functions, as well as to the $\Phi_i(\mathbf{x}_1, \dots, \mathbf{x}_N)$, must be contained inside the R-matrix sphere. The coefficients a_{ijk} and b_{ik} are obtained by diagonalizing, in the inner region, the matrix of elements $(\Psi_k^\Gamma | \mathcal{H} - \mathcal{L} | \Psi_{k'}^\Gamma)$. \mathcal{L} is the Bloch operator¹⁴ necessary to ensure hermiticity.

In the outer region, the scattering electron is distinguishable from the target electrons and exchange and correlation effects can be neglected. The interaction potential can be described in terms of a single-centre multipole expansion (permanent and transition dipole and quadrupole moments are considered; polarization effects are not). Therefore, the set of coupled differential equations to be solved are simpler. The inner region data is used as boundary conditions to solve the outer region problem using a propagation technique¹⁴. Matching the asymptotic solutions to known expressions, the K-matrix and S-matrix and thus resonance parameters and cross sections, can be determined.

The choice of functions describing target, $\Phi_i(\mathbf{x}_1, \dots, \mathbf{x}_N)$ (i.e. how many and calculated and at what level of approximation) and L^2 functions of (1) determines the scattering model. In the SE model, only the ground state is considered and relaxation of the target in the presence of the scattering electron is not described. A Hartree-Fock (HF) description of the

ground state is used. In the SEP model, $N+1$ configurations involving single excitations from the ground state are used to describe close-range correlation-polarization effects (the target is described as in the SE model, with only the ground state considered). The L^2 functions take the form:

$$\chi_i^{SEP} : (\text{core})^{N_d}(\text{valence})^{N-N_d-1}(\text{virtual})^{1+1}, \quad (2)$$

where N_d is the number of frozen electrons. The valence orbitals are those occupied in the ground state HF configuration from which single excitation are allowed. There is no simple way to choose the optimal number of virtual orbitals (v.o.), as it is not possible to quantify how much polarization the L^2 functions describe. If too many are used the calculations can be 'overcorrelated' and the resonances will appear lower in energy than in the experiment¹⁵.

In the Close-Coupling (CC) model, the target can be electronically excited and a number states (described at the CASSCF level in this work) are included in (1). Inclusion of excited state describes some of the polarization effects, but for targets with high polarizability, additional L^2 functions must be included. The L^2 functions take the form:

$$\chi_i^{CC} : \begin{cases} (\text{core})^{N_d}(\text{CAS})^{N-N_d+1}, \\ (\text{core})^{N_d}(\text{CAS})^{N-N_d}(\text{virtual})^1, \end{cases} \quad (3)$$

where CAS denotes the orbitals of the active space. Note that in this case 'virtual' refers to orbitals that are neither frozen nor included in the active space (this set is therefore different to that of the 'virtual' orbitals in a SE/SEP calculation).

In order to identify and characterize resonances, we have calculated and analyzed the time-delay¹⁶ obtained from the S-matrix. This has been shown to be a more effective approach than the use of the eigenphase sum for targets with a large dipole moment and/or where a large number of resonances are present¹⁷.

In this work we have used the UKRmol+ suite, a parallelized, re-engineered version of the R-matrix suite UKRmol¹⁸. The crucial improvement in the UKRmol+ suite is the ability to compile and run the codes with quadruple precision. This enabled us to use larger R-matrix radii without the need to delete significant number of continuum orbitals in the orthogonalization step¹⁵ and include higher partial waves in the continuum description.

CHARACTERISTICS OF THE CALCULATIONS

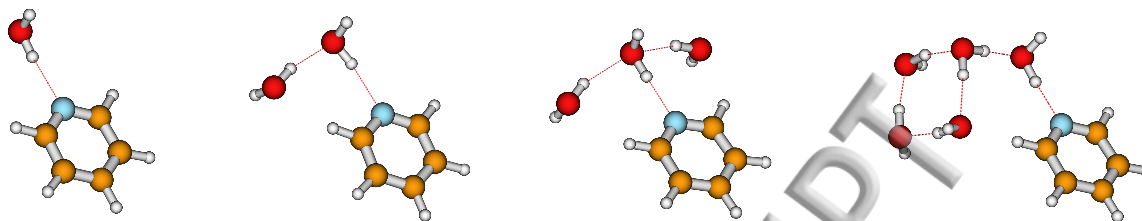


FIG. 1: Optimized ground state geometries of the Pyr-(H₂O)_n clusters studied in this work for $n = 1, 2, 3$ (adapted from Schlücker *et al.*¹⁹, see main text) and $n=5$ (Sicilia *et al.*²⁰). The coloured balls represent: blue - nitrogen; orange - carbon; red - oxygen and white - hydrogen. The red lines indicate the hydrogen bonds. Plots generated using MOLDEN.

The ground state equilibrium geometry of isolated pyridine used in the calculations was taken from the CCCBDB database, we chose that optimised at the QCISD level²¹. The optimized geometry of the clusters Pyr-H₂O, Pyr-(H₂O)₂, Pyr-(H₂O)₃ were generated by optimizing (with MOLPRO) an initial geometry constructed from parameters provided by Schlücker *et al.*¹⁹ (geometrical parameters of the water molecules and their relative position to the ring) and the above-mentioned geometry of pyridine. The geometry of the Pyr-(H₂O)₅ system comes from Sicilia *et al.*²⁰. Figure 1 shows all the clusters studied in this work.

For the SE calculations, the ground state of all clusters was described at HF level using the cc-pVDZ basis set. The relevant properties of these clusters and isolated pyridine and water obtained in this work are collected in Table I, together with experimental and other calculated values where available. The Pyr-(H₂O)_n clusters with $n > 1$ have not been broadly studied so far. Therefore, no data was found to compare our calculated target properties for the larger systems. Our results for Pyr-H₂O show reasonable agreement with a previous calculated value of the dipole moment. Our calculated energies are, as expected, higher than those from better calculations.

For the CC calculations the ground and excited states were described using a state-averaged CASSCF model and the cc-pVDZ basis set. In the case of pyridine the active space comprised 10 electrons that are allowed to occupy 8 orbitals: CAS(10,8). For Pyr-H₂O we used a CAS(12,9) active space (this is the largest one for which calculations could be performed).

We restricted our CC calculation to 9 states (the ground state and 8 excited states) in order to include only excited states linked to pyridine and to make sure these were the same for both targets. All 9 states were used in the state-averaging.

	H ₂ O	Pyr	Pyr-H ₂ O	Pyr-(H ₂ O) ₂	Pyr-(H ₂ O) ₃	Pyr-(H ₂ O) ₅
P.G.	C_{2v}	C_{2v}	C_s	C_1	C_s	C_1
E	-76.027 -76.233 ^a	-246.714 -247.537 ^a	-322.752 -323.783 ^a	-398.795	-474.833	-626.905
μ	2.01 2.28 ^a 1.85 ^c	2.22 2.46 ^a 2.19 ^d	4.68 4.27 ^b	3.46	2.70	6.57
α	9.67 ^e 10.13 ^g 9.78 ^h	60.00 ^f 64.06 ^g 64.10 ⁱ	68.16 ^f			

TABLE I: Structural and electrostatic properties of the electronic ground states of water, pyridine and Pyr-(H₂O)_n. Listed are: point group (P.G.), energy (E) in Hartree, dipole moment (μ) in Debye and spherical polarizability (α) in atomic units (a_0^3). Bold values: this work (see text for details). ^a Calculated at MP2/6-31++G** level²². ^b Calculated at MP2/cc-pVDZ level²⁰. ^c Calculated at MP2/aug-cc-pVQZ level²¹. ^d Calculated at MP2/6-31+G(d) level²³. Experimental values: c^{24} , d^{25} , g^{21} , h^{26} , i^{27} .

The scattering calculations were carried out with an R-matrix radius $a = 15a_0$ for Pyr-H₂O, Pyr-(H₂O)₂ and Pyr-(H₂O)₃ and $a = 18a_0$ for Pyr-(H₂O)₅. The continuum basis set included partial waves up to $\ell_{max} = 6$ in all cases. Results were obtained at SE levels for all clusters, while SEP (not presented in this paper) and CC calculations were also performed for Pyr-H₂O.

When polarization effects are not included in the calculation (as is the case for the SE approximation) most resonances appear at significantly higher energies than experimentally; the resonance parameters, i.e. positions, widths, tend to be qualitative rather than quantitative. Nonetheless, at the moment, SE calculations are the most appropriate to investigate changes to the resonances due to hydration with our R-matrix approach. Inclusion of polarization at SEP and CC levels (in the latter case, particularly when the second type of L^2

function in (3) are included) cannot be done in a 'converged' manner. Since, in addition, it is not possible to quantify how much polarization is being described by a specific calculation, we are unable to either determine the optimal set of L^2 configurations to include or to ensure that the same amount of polarization is included in different calculations. In the past, for similar molecules (e.g. pyrimidine and uracil) we have used agreement with experimental positions of the low-lying π^* resonances as the way to determine the best set of L^2 configurations¹⁷. We have then used the experience gained from these systems to determine the best approach for molecules of the same family (e.g. other diazines). Since no prior data is available for the resonances of microhydrated diazines or similar targets, we are unable to adopt this approach in this case. This means that it is not possible to confidently obtain quantitative energy shifts from a comparison of the resonances positions from SEP or CC calculations.

Freitas *et al.* have shown that calculations at SE and SEP levels give the same qualitative description of the changes to resonance in formaldehyde and formic acid due to hydrogen bonding to one and two water molecules^{4,5} (the shifts of the resonance were quantitatively different: differences can go up to 0.6 eV, though they tend to be smaller; in general, it's the SEP approximation that produces larger shifts). We expect that SE calculations will therefore be sufficient to get semi-quantitative ideas of how resonances are affected by microhydration. We have, nonetheless, performed SEP and CC calculations where we estimate we have a similar amount of polarization description for the isolated target and the cluster. Although less reliable, these results do provide an insight into the effect of hydration on resonances, especially the CC ones where core-excited resonances are described. No prior work has, to our knowledge, looked at the effect of microhydration on core-excited resonances.

IV. RESULTS

We will mainly concentrate on the two lowest (purely shape) resonances in pyridine¹². These are π^* resonances that have been clearly identified and characterized computationally and are expected to appear in experiments below 2 eV^{28,29}. The first resonance belongs to the B_1 irreducible representation whereas the second one belongs to A_2 . A third π^* resonance (again, of B_1 symmetry), of mixed shape-core excited character, is also visible in some of

figures below, but we have not studied it in detail as SE calculations do not describe these mixed resonances accurately. We note that water does not possess shape resonances in the low energy range (at least for the geometries involved in the clusters studied here).

A. Direct and indirect effects

Investigating shape resonances in microhydrated molecules in detail, we realised that the effect of water on the resonance positions can be better analysed if it is separated into two contributions. We therefore distinguish direct and indirect effects, whose definitions are given below.

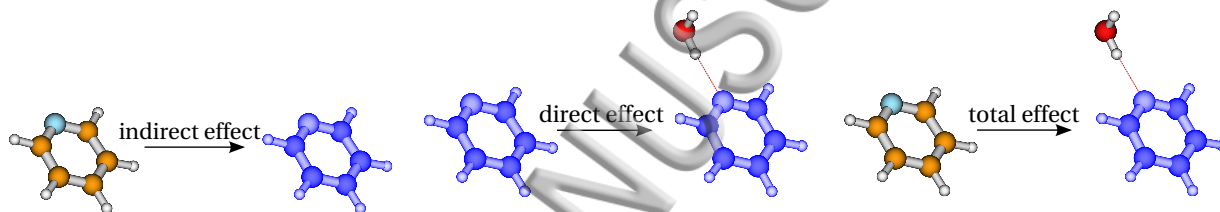


FIG. 2: Schematic illustration of the systems compared to investigate indirect, direct and total effects of microhydration on the resonances of pyridine. The picture of pyridine in 'natural' colours symbolises pyridine in its isolated, ground state, equilibrium geometry; the blue colour indicates pyridine being investigated in the optimized geometry of the cluster.

A study of these effects together with the total effect (the sum of direct and indirect effects) gives a better insight into the influence of water on resonances. The effects, schematically described in Figure 2, are as follows:

- Indirect effect: due to the changes to the molecular (here pyridine) geometry that result from binding with water. These effects are therefore observed by comparing the resonances of the target molecule in two different geometries but *without* the inclusion of water in the calculations. These are the ground state equilibrium geometry of the isolated molecule and that of the molecule in the optimized geometry of the cluster. With few exceptions, the geometry of molecules in the clusters investigated by us differs from the equilibrium geometry. If the geometry of the molecule in a cluster is sufficiently different³⁰ from its equilibrium one, the resonance positions are shifted.

- Direct effect: due to the presence of water but excluding the changes caused by differences in geometries. The effect is observed comparing the resonance characteristics for the isolated molecule *in the geometry it has in the cluster* and the cluster (here pyridine and Pyr-(H₂O)_n). Therefore, the geometry of the molecule (pyridine) is the same in both systems (see Figure 2).
- Total effect: the total effect of microhydration can be determined by adding direct and indirect effects. This corresponds to comparing resonance characteristics for isolated molecule and cluster (pyridine and Pyr-(H₂O)_n) in their equilibrium geometries (see Figure 2).

It should be noted that previous work discussed (implicitly) a mix of direct and total effects: the calculations for formic acid⁵ used the equilibrium geometry of isolated HCOOH in the clusters. Therefore their results do not take into account indirect effects (but can't be equated to our direct effects either). Those for phenol investigate the total effects⁶ (the geometries of the clusters were optimized for the liquid phase using Monte Carlo simulations) and that is probably also the case for formamide⁴.

B. Pyridine-H₂O: shape resonances

Pyr-H₂O belongs to the C_s point group; the three low-lying π^* resonances of pyridine have the following C_s symmetry (in energy order): A', A'' and A'. Figure 3 shows the time-delay for isolated pyridine in both equilibrium (Pyr Eq) and cluster (Pyr 1w) geometries and for the Pyr-H₂O cluster. Comparing the first two we can analyze the indirect effect: all three resonances visible in the figure are slightly destabilized by the change of geometry caused by water bonding to pyridine. Comparing Pyr 1w with Pyr-H₂O we can see that the direct effect leads to the stabilization of all visible resonances. Since, in this case, the indirect effect is smaller than the direct effect, the total effect due to the presence of water is that of stabilizing the resonances. The relatively small differences in the resonance positions of isolated pyridine and Pyr-H₂O in their equilibrium geometries visible in Figure 3 indicates the effect is small. The first shape resonance (1 ²B₁ or 1 π^* resonance) is shifted to lower energy by about 0.24 eV. The second (1 ²A₂ or 2 π^* resonance) is shifted to lower energy by about 0.21 eV. (At the SEP level, the size of the shifts is somewhat bigger, and dependent on

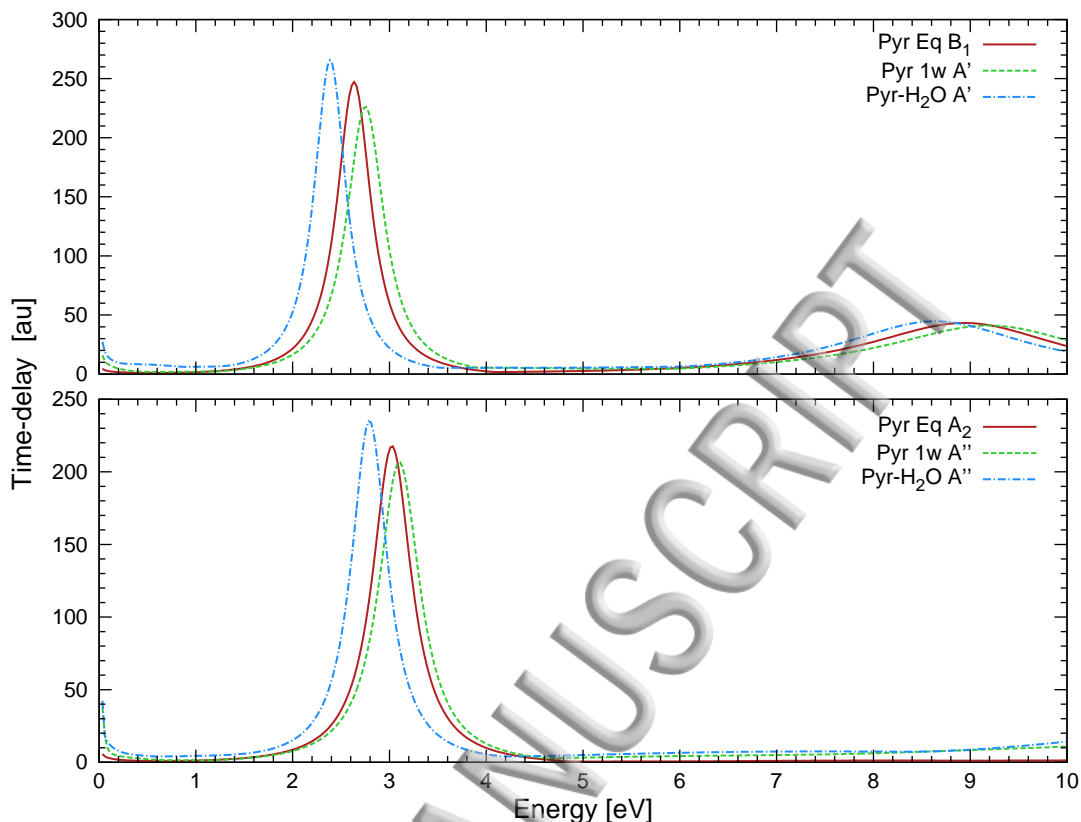


FIG. 3: Time-delay for isolated pyridine in its equilibrium geometry (Pyr Eq), isolated pyridine in its cluster geometry (Pyr 1w) and Pyr-H₂O in its optimized geometry calculated at SE level. The time-delay is plotted for the symmetries indicated in the panel.

the number of v.o. included in the calculation. This is consistent with the results for formic acid where the shift increases from 0.5 to 0.6 eV in going from SE to SEP calculations⁵.)

C. Pyridine-H₂O: core-excited resonances

The ground state and 8 excited states are included in all CC calculations presented in this Section. These excited states correspond to excitation of pyridine only (i.e. the H₂O molecule in the cluster remains in its ground state). For this reason, no resonance that could be associated to water excitation is described. (Isolated water has two Feshbach resonances that should be visible in this energy range³¹.) This rather small CC calculation does not describe the resonances very accurately. A detailed description of the resonance spectrum of isolated pyridine will be published elsewhere.

The CC calculations presented in Figure 4 were performed using 0 virtual orbitals (there-

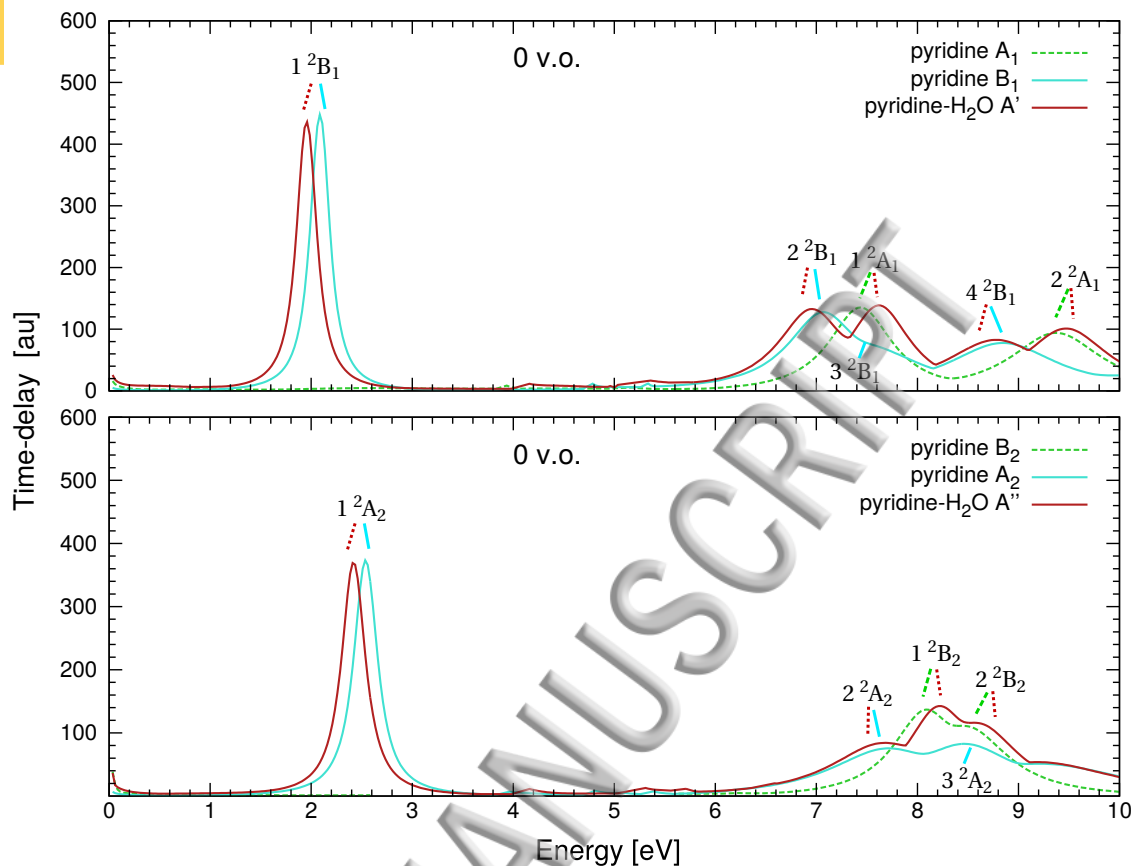


FIG. 4: Time-delay for pyridine (in its equilibrium geometry, Pyr Eq) and Pyr-H₂O for the symmetries indicated in the panels calculated at CC level. See main text for details of the calculations. The resonances present, and their symmetries, are indicated in both panels.

fore, the second type of L^2 function in (3) are not present)³². The Figure shows that, overall, all resonances visible in the time-delay for pyridine are also visible for Pyr-H₂O. In agreement with the SE and SEP calculations, the pure shape resonances are slightly shifted to lower energy in the presence of water. This is also the case for some of the core-excited (and mixed shape-core-excited) resonances but not for all. The $1\ ^2A_1$ and $2\ ^2A_1$ resonances (at ~ 7.6 eV and ~ 9.5 eV in the A' symmetry for Pyr-H₂O) and $1\ ^2B_2$ and $2\ ^2B_2$ resonances (at ~ 8.2 eV and ~ 8.6 eV in A'' symmetry for Pyr-H₂O) of Pyr-H₂O are shifted to higher energy compared to isolated pyridine by about 0.1-0.2 eV. These resonances have a pure core-excited character. It can also be noted that an extra peak is visible for pyridine at ~ 7.5 eV ($3\ ^2B_1$ resonance) very close to another one at ~ 7.1 eV ($2\ ^2B_1$ resonance). This resonance cannot be seen in Figure 4 but is present in Pyr-H₂O: due to the lower symmetry of the system this peak is hidden by another one. A similar situation can be noticed for the

2^2A_2 resonance.

As expected, inclusion of polarization in the calculations lowers all of the resonances visible in Figure 4. Calculations for isolated pyridine including 9 target states showed that 80 v.o. (selected in energy order) were appropriate to describe the resonances accurately. Therefore, we performed calculations in which we included these same 80 v.o. (picked by visual inspection) in addition to all other orbitals whose energies were in this orbital energy range in the Pyr-H₂O calculation. We expect therefore to have a similar description of the polarization of pyridine in both cases (and some description of the polarization of water; we note that the polarizability of water is approximately 6 times smaller than that of pyridine).

These calculations are presented in Figure 5. All resonances are now stabilized. The majority of the resonance shifts are approximately between 0.3 eV and 0.4 eV. For the resonances 1^2A_1 , 2^2A_1 , 1^2B_2 and 2^2B_2 the shifts are not higher than 0.13 eV.

Inclusion of polarization has, as expected, a stabilizing effect. This means that resonances that appear to be destabilized (total effects) may become stabilized when more polarization is included. We conclude that the effect of microhydration on the core-excited resonances is similar to that on shape resonances.

D. Pyridine-(H₂O)_n, n=2,3,5

All calculations presented in this section have been performed at SE level. For these clusters, we only show the indirect and total effects of microhydration (the direct effects can be easily derived as the difference between them).

Figure 6 illustrates the equilibrium geometry of isolated pyridine (Pyr Eq) and its geometry in the cluster with five water molecules (Pyr 5w). The changes in bond-lengths between these systems are smaller than $\sim 1.4\%$. We note that the geometry of pyridine in all clusters presented in this paper differs less than $\sim 0.2\%$ from that of Pyr-(H₂O)₅. This small effect of additional waters is probably due to the fact that these don't attach to pyridine but to other waters. As a result, the comparison of the time-delay for pyridine in its isolated equilibrium geometry and in the geometry in the different clusters is very similar to that presented in section IV B. In other words, the indirect effect of microsolvation changes very little with additional waters.

Figure 7 shows the two lowest π^* resonances for isolated pyridine and Pyr-(H₂O)_n, n=1,

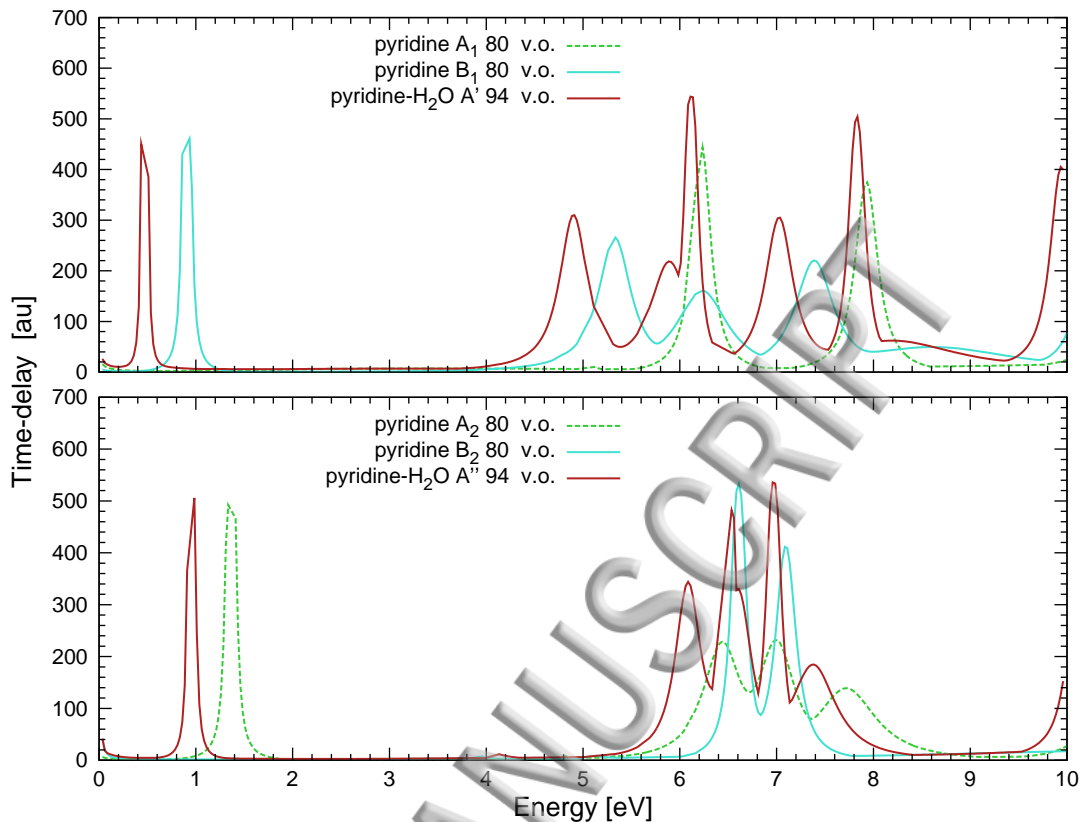


FIG. 5: The time-delay for pyridine (in its equilibrium geometry, Pyr Eq) and Pyr-H₂O calculated at CC level for the number of virtual orbitals indicated in the panels; the time-delay is plotted for the symmetries indicated.

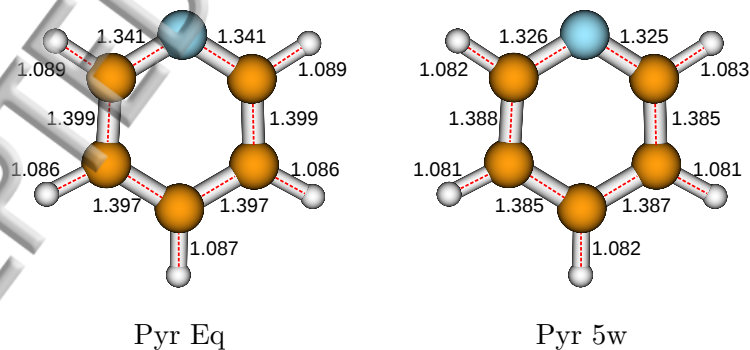


FIG. 6: Bond-lengths, in Å, of pyridine in its equilibrium geometry (Pyr Eq) and in the optimized geometry of the cluster with 5 water molecules (Pyr 5w).

2, 3, 5. Note that the irreducible representations have been summed or plotted in both panels, as appropriate, to facilitate the comparison (see the legend of the figure for details). For all these systems water stabilizes these resonances. Therefore, we once again observe that

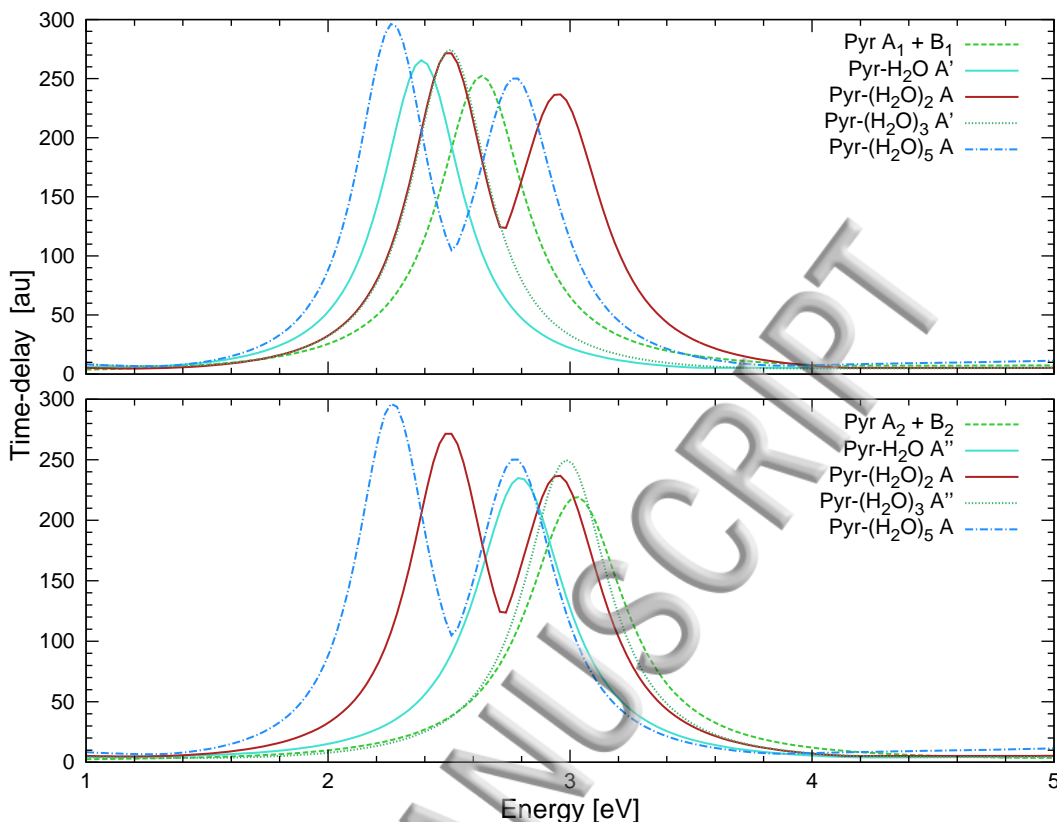


FIG. 7: Time-delay for pyridine and $\text{Pyr}-(\text{H}_2\text{O})_n$, $n=1, 2, 3, 5$ for the symmetries indicated in the panels. To ease comparison the contribution to the time-delay of two irreducible representations is summed for pyridine in each panel. The time-delay for the clusters with no symmetry ($\text{Pyr}-(\text{H}_2\text{O})_n$, $n=2,5$) is plotted in both panels: therefore, care should be taken with comparing the appropriate peak in each case. All calculations were performed at SE level.

whereas the indirect effect (illustrated in Figure 3 for $\text{Pyr}-\text{H}_2\text{O}$) destabilizes the resonance slightly, the direct effect has a stronger stabilization effect and, as a result, the resonances are stabilized by microhydration. The shifts are not significant, especially for $\text{Pyr}-(\text{H}_2\text{O})_2$ and $\text{Pyr}-(\text{H}_2\text{O})_3$ where the shift is smaller than for $\text{Pyr}-\text{H}_2\text{O}$. The biggest change in resonance position occurs for $\text{Pyr}-(\text{H}_2\text{O})_5$.

We can see that the stabilization effect is stronger for the first π^* resonance than the second for all clusters presented in this work: the largest difference is observed for $\text{Pyr}-(\text{H}_2\text{O})_5$ where the magnitude of shifts is 0.36 and 0.26 eV respectively; the smallest for $\text{Pyr}-\text{H}_2\text{O}$, where they are 0.25 and 0.21 eV respectively. These differences can be attributed

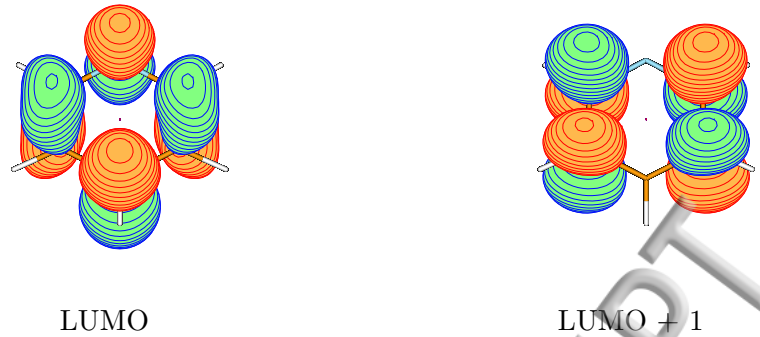


FIG. 8: The LUMO (b_1 symmetry) and LUMO + 1 (a_2 symmetry) of pyridine in its ground state equilibrium geometry.

to the different electronic density around the nitrogen atom for the π^* orbitals that are occupied by the electron in these resonances. The electronic density associated to them is shown in Figure 8 for isolated pyridine (these orbitals are very similar in all clusters and the isolated molecule). The nitrogen atom participates in the hydrogen bonding as the hydrogen-acceptor and the hydrogen of one water molecule points towards it in all clusters. The first of these orbitals has significant density around the nitrogen, whereas the second one has hardly any density associated to it. This probably explain the slightly stronger stabilization from a purely electrostatic point of view: the slightly positive hydrogen atom from the nearby water has a stronger effect on the orbital that describes more density close to it.

V. DISCUSSION AND CONCLUSIONS

The SE calculations presented in this work for Pyr-(H₂O)_n n=1,2,3,5 have allowed us to investigate the effect of microhydration on the two lowest, shape, resonances of pyridine. The results provide a clear description of how changes to the static and exchange potentials experienced by the scattering electron affect the resonances. The results confirm the conclusions obtained by of Freitas, Bettega and collaborators⁴⁻⁶ using the Schwinger Multichannel method: water acting as a hydrogen donor stabilizes the resonances.

The resonance shifts for the clusters are connected with the energy of the orbitals to which the electron binds for the two π^* resonances: the energy differences between the orbitals of the clusters and isolated pyridine are close to the resonance shifts. The trend of the shifts

is correlated with the dipole moments of the clusters: the bigger the dipole moment, the bigger the shift. If, for simplicity, we assume that dipole moment of pyridine in the cluster is approximately equal to that of isolated pyridine, then a total dipole moment larger than that of isolated pyridine indicates that the water molecules are responsible for the increase. Since the water molecules attach to the more electronegative part of pyridine, this bigger dipole moment implies that more of the electronic density is on the water molecules and away from the ring. This leads to a stronger attraction of the scattering electron to the cluster than to isolated pyridine: the resonances are stabilized. The opposite happens when the total dipole moment of the cluster is smaller than that of isolated pyridine: more negative charge is next to the ring, making it is less attractive for the incoming electron.

In addition, CC calculations have shown that the same effect is observed for core-excited resonances. Changes to the amount of polarization included in the CC calculations lead to different qualitative behaviour for some of the resonances: these appeared to be destabilized when little of the polarization was included in the calculations, but were stabilized when more polarization was described. Since, as explained above, we are not able to quantify the amount of polarization included in our calculations, it is not possible to be completely confident that calculations that include more polarization provide a better comparison between systems and therefore a better description of the shifts. Increased polarization description will always lead to the shifting of shape resonances to lower energy. How much, however, will depend on the system. It is therefore possible, though we believe unlikely, that in our biggest CC calculations polarization is better described for the cluster than the isolated molecule: this would lead to the cluster resonances being 'too low' relative to the isolated molecule ones, giving the impression that all resonance are stabilized when this is not the case.

In the case of the shape resonances, SEP calculations (not shown in the paper) for various numbers of virtual orbitals indicate that the resonances are stabilized and that this is the case for different amounts of polarization.

We have interpreted the consequences of microhydration on the resonances in terms of a direct and indirect effect. The indirect effect is similar for all of the clusters studied and leads to a small destabilization of the resonances. It is possible (though we have not looked at it) that in the SEP calculations the indirect effect is stabilizing (in thymine-(H₂O)₅, where we have looked at this (see Paper II), the indirect effects are stabilizing at both SE and SEP levels).

The direct effect is stronger and leads to stabilization. As a result, the total microhydration effect leads to the stabilization of the resonances. This result raises the possibility that, in some 'extreme' cases, the total effect of a water molecule being the hydrogen donor in the bond might actually lead to destabilization of the resonances.

In conclusion, this study shows that in the case of pyridine, hydration leads to the stabilization of all resonances present in the system. The resonance shifts are small and different for different resonances. More accurate calculations, particularly those including an accurate description of polarization, are needed to provide a more quantitative picture of the hydration effects.

VI. SUPPLEMENTARY MATERIAL

Plots of SE elastic cross section for pyridine and Pyr-(H₂O)_n n=2, 3 and 5 and CC total (summed over the 8 electronically excited states included in the calculation) inelastic cross section for pyridine and Pyr-H₂O are presented in the supplementary material.

VII. ACKNOWLEDGEMENTS

We are grateful to Profs. Alfonso Niño and Camelia Muñoz-Caro for providing the geometry of the pyridine-(H₂O)₅ cluster. This work used the ARCHER UK National Supercomputing Service (<http://www.archer.ac.uk>).

REFERENCES

- ¹I. Baccarelli, I. Bald, F. A. Gianturco, E. Illenberger, and J. Kopyra, *Phys. Rep.* **508**, 1 (2011).
- ²B. Boudaïffa, P. Cloutier, D. Hunting, M. A. Huels, and L. Sanche, *Science* **287**, 1658 (2000).
- ³J. D. Gorfinkiel and S. Ptasińska, *J. Phys. B* (submitted).
- ⁴T. C. Freitas, M. A. P. Lima, S. Canuto, and M. H. F. Bettega, *Phys. Rev. A* **80** (2009), 10.1103/PhysRevA.80.062710.
- ⁵T. C. Freitas, K. Coutinho, M. Varela, M. A. P. Lima, and S. Canuto, *J. Chem. Phys.* **138** (2013), 10.1063/1.4803119.

- ⁶E. M. De Oliveira, T. C. Freitas, K. Coutinho, M. T. Márcio, S. Canuto, M. A. P. Lima, and M. H. F. Bettega, *J. Chem. Phys.* **141** (2014), 10.1063/1.4892066.
- ⁷M. Neustetter, J. Aysina, F. F. daSilva, and S. Denifl, *Angew. Chem., Int. Ed.* **54**, 9124 (2015).
- ⁸J. Kočišek, A. Pysanenko, M. Fárník, and J. Fedor, *J. Phys. Chem. Lett.*, 3401 (2016).
- ⁹M. Smyth, J. Kohanoff, and I. Fabrikant, *J. Chem. Phys.* **140** (2014), 10.1063/1.4874841.
- ¹⁰I. I. Fabrikant, S. Caprasecca, G. A. Gallup, and J. D. Gorfinkiel, *J. Chem. Phys.* **136**, 184301 (2012).
- ¹¹A. Sieradzka and J. D. Gorfinkiel, *J. Chem. Phys.* (2017).
- ¹²A. Sieradzka, F. Blanco, M. C. Fuss, Z. Mašín, J. D. Gorfinkiel, and G. García, *J. Phys. Chem. A* **118**, 6657 (2014).
- ¹³A. S. Barbosa, D. F. Pastega, and M. H. F. Bettega, *Phys. Rev. A* **88**, 022705 (2013).
- ¹⁴P. G. Burke, *R-Matrix Theory of Atomic Collisions: Application to Atomic, Molecular and Optical Processes* (Springer, 2011).
- ¹⁵J. Tennyson, *Phys. Rep.* **491**, 29 (2010).
- ¹⁶F. T. Smith, *Phys. Rev.* **118**, 349 (1960).
- ¹⁷Z. Mašín and J. D. Gorfinkiel, *J. Chem. Phys.* **137**, 204312 (2012).
- ¹⁸J. M. Carr, P. G. Galiatsatos, J. D. Gorfinkiel, A. G. Harvey, M. A. Lysaght, D. Madden, Z. Mašín, M. Plummer, J. Tennyson, and H. N. Varambhia, *Eur. Phys. J. D.* **66** (2012), 10.1140/epjd/e2011-20653-6.
- ¹⁹S. Schlücker, R. K. Singh, B. P. Asthana, J. Popp, and W. Kiefer, *J. Phys. Chem. A* **105**, 9983 (2001).
- ²⁰M. C. Sicilia, C. Muñoz Caro, and A. Niño, *ChemPhysChem* **6**, 139 (2005).
- ²¹R. D. Johnson III Editor, “NIST Standard Reference Database Number 101,” <http://cccbdb.nist.gov/> (2011).
- ²²A. Dkhissi, L. Adamowicz, and G. Maes, *J. Phys. Chem. A* **104**, 2112 (2000).
- ²³E. Fileti, K. Coutinho, T. Malaspina, and S. Canuto, *Phys. Rev. E* **67**, 061504 (2003).
- ²⁴S. Clough, Y. Beers, G. Klein, and L. Rothman, *J. Phys. Chem.* **59**, 2254 (1973).
- ²⁵R. D. Nelson Jr., D. R. Lide, and A. A. Maryott, “Selected values of electric dipole moments for molecules in the gas phase,” Tech. Rep. (NSRDS-NBS10, 1967).
- ²⁶D. R. Lide, *Handbook of Chemistry and Physics* (CRC Press, Boca Raton, FL, 1994).
- ²⁷C. Lefevre, R. Lefevre, B. Rao, and M. Smith, *J. Chem. Soc.*, 1188 (1959).

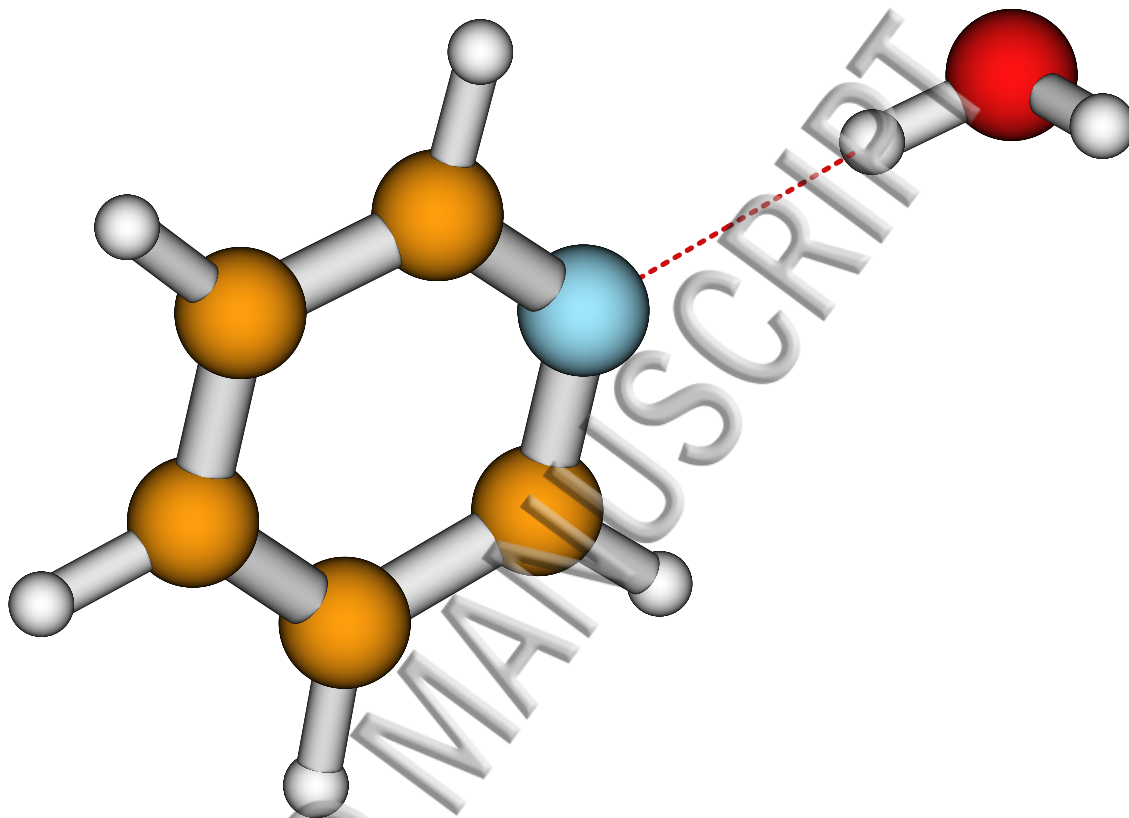
²⁸F. Nenner and G. J. Schulz, J. Chem. Phys. **62**, 1747 (1975).

²⁹A. Modelli and P. Burrow, J. Electron Spec. **32**, 263 (1983).

³⁰For pyridine and thymine (see Paper II) the changes in resonance positions are observable if at least six bonds differ by at least ~ 0.01 Å; changes to the bonds not associated to the ring are also significant.

³¹J. D. Gorfinkiel, L. A. Morgan, and J. Tennyson, Journal of Physics B: Atomic, Molecular and Optical Physics **35**, 543 (2002).

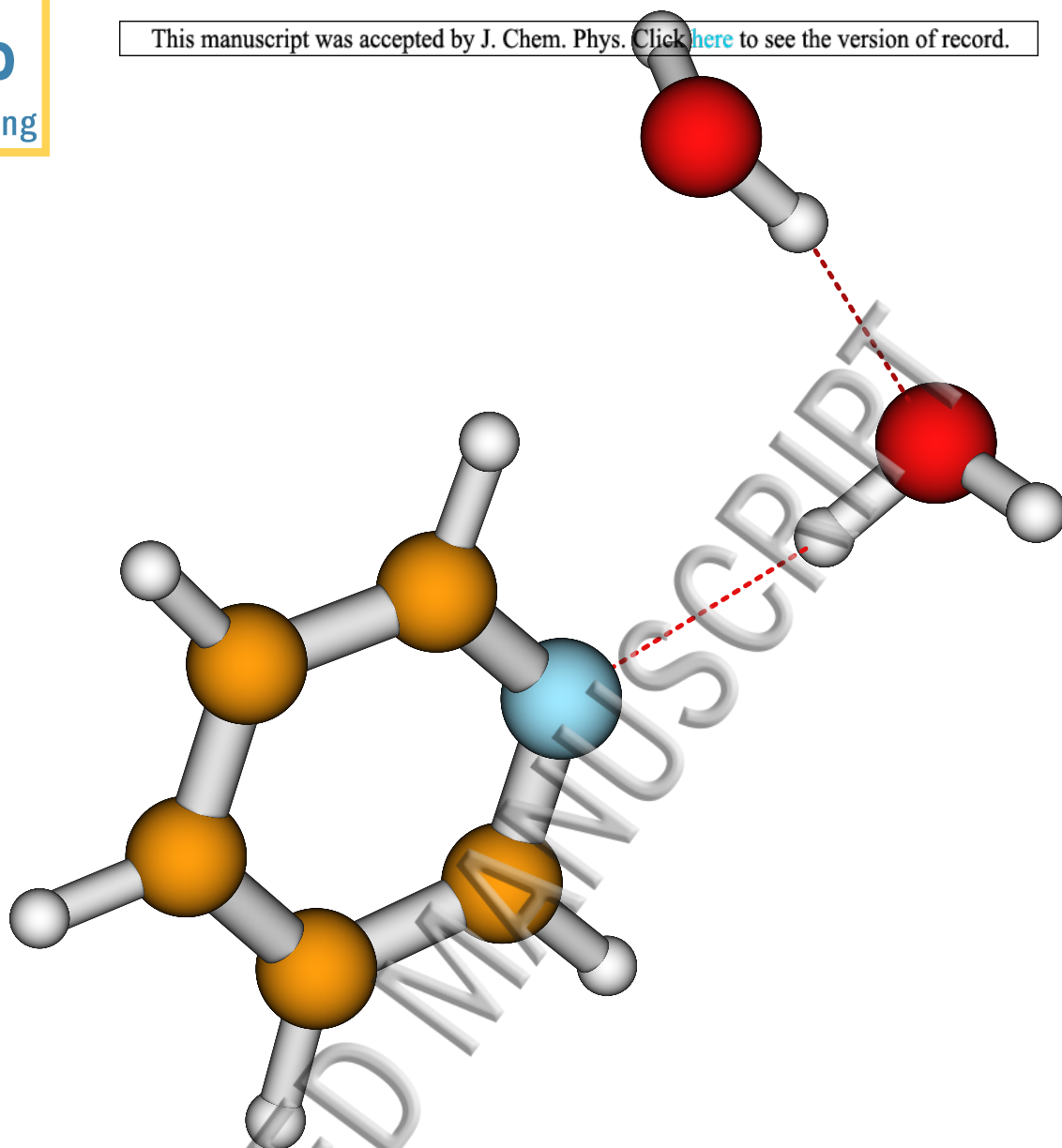
³²The CC calculations with 0 v.o. do include some amount of polarization described by the target excited states included and the first type of L^2 functions. Therefore, whereas one can confidently say that in SE calculations the comparison is like with like (but not in the SEP calculations), for the CC ones this is not possible.



single point

defaults used

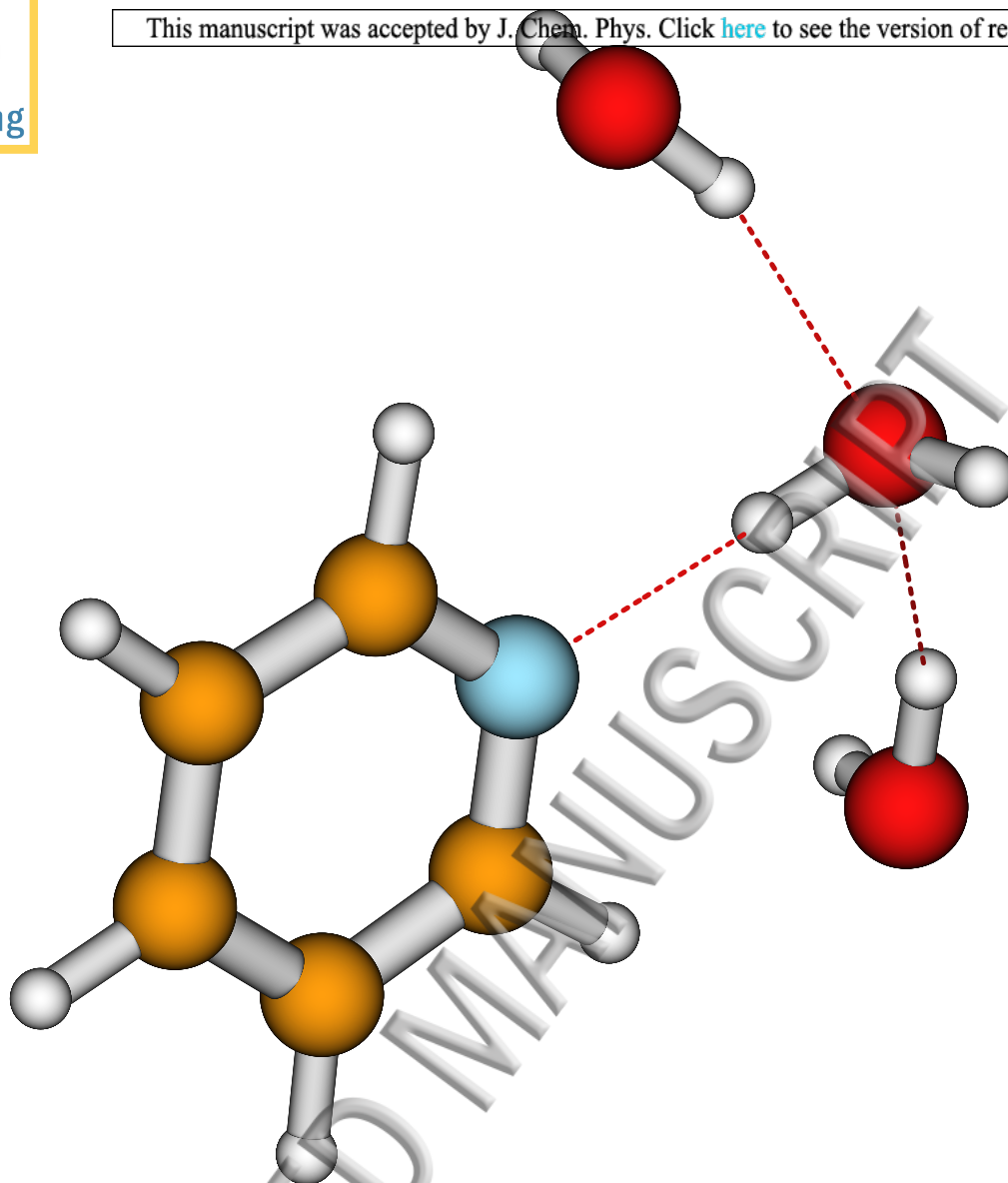
MOLDEN



single point

defaults used

MOLDEN

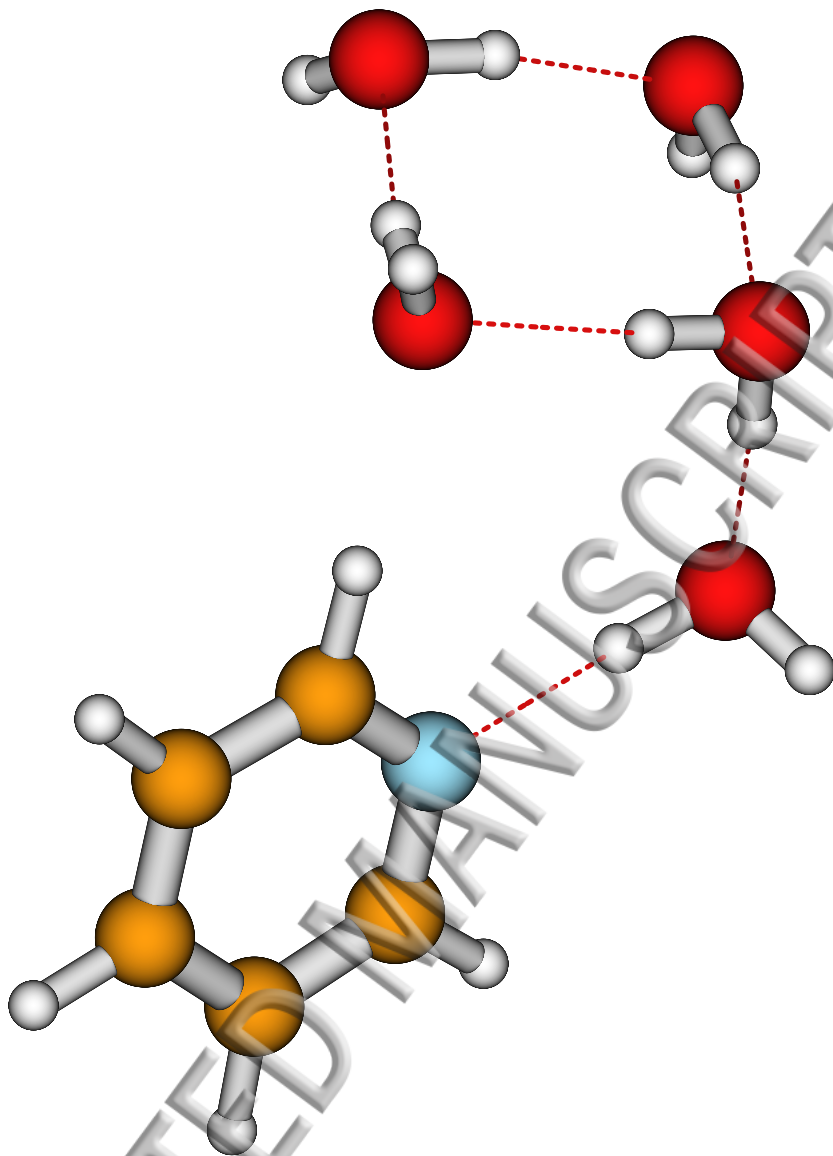


single point

defaults used

MOLDEN

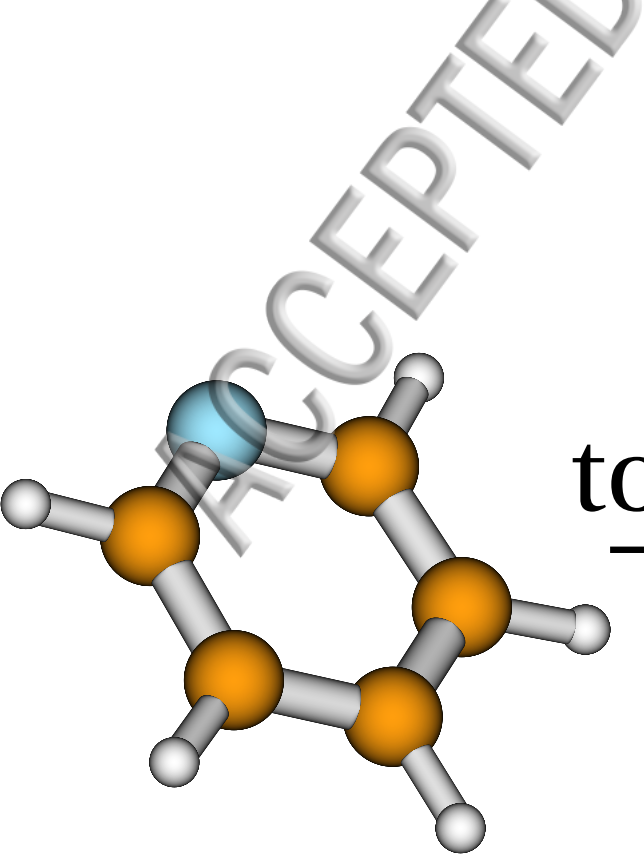
ACCEPTED MANUSCRIPT



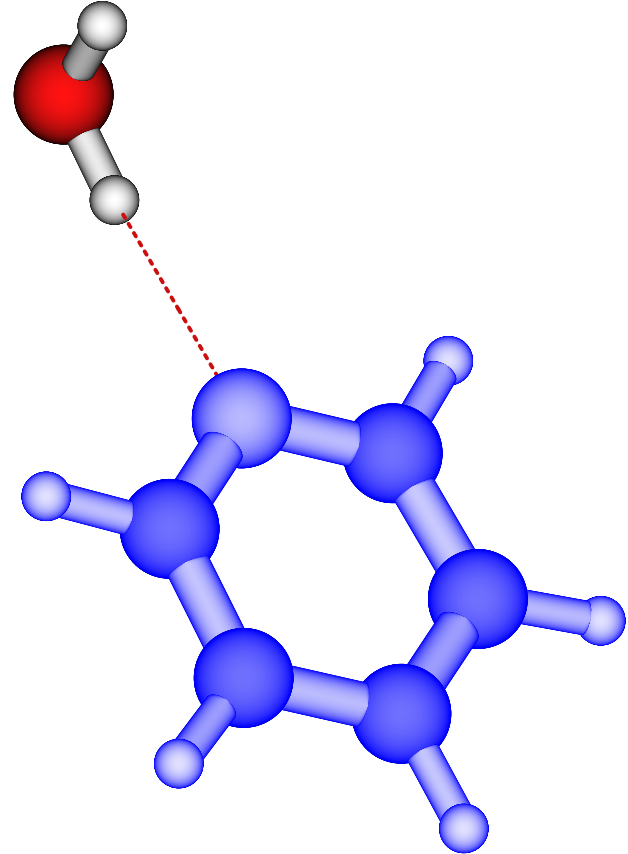
single point

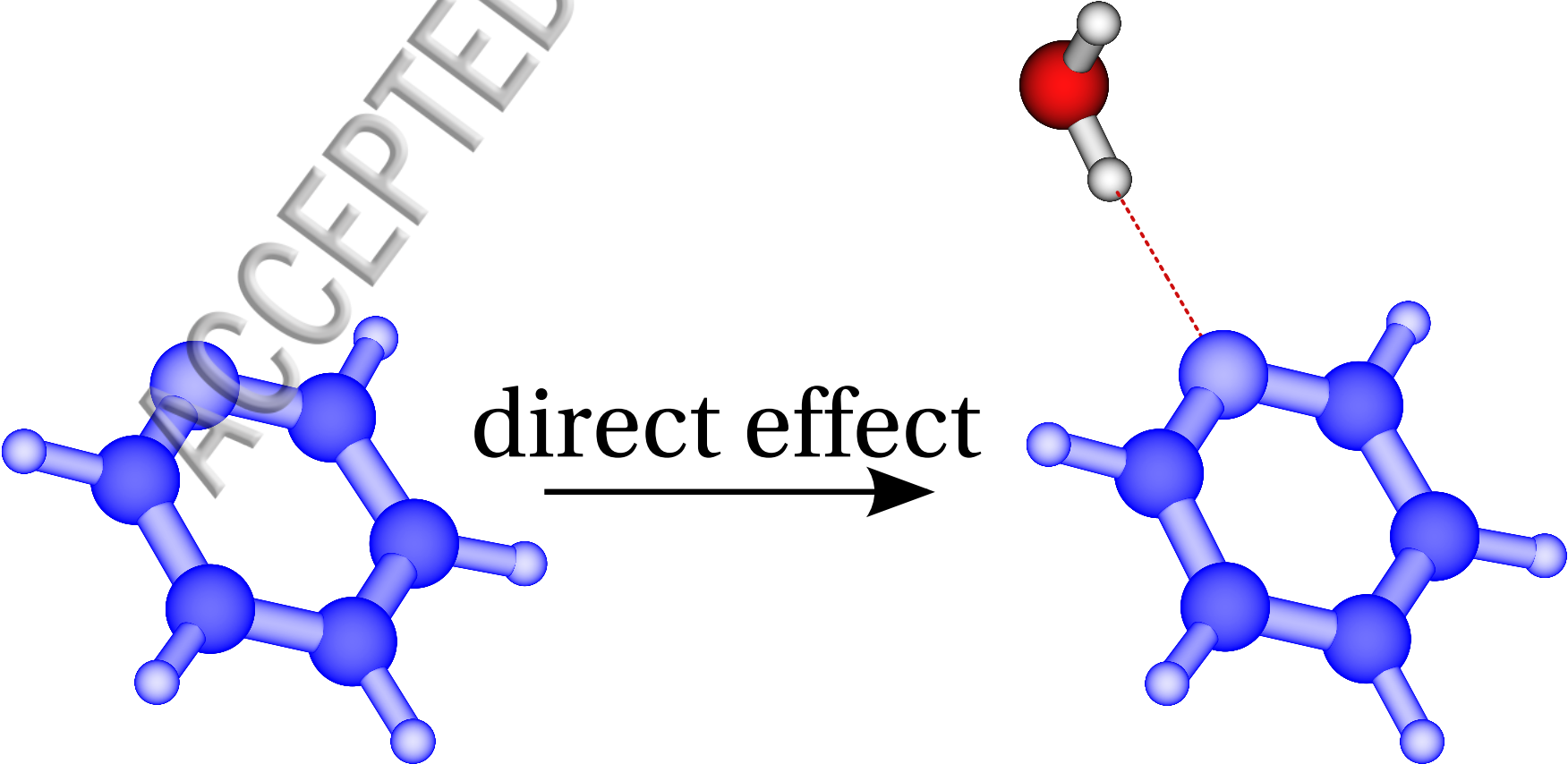
defaults used

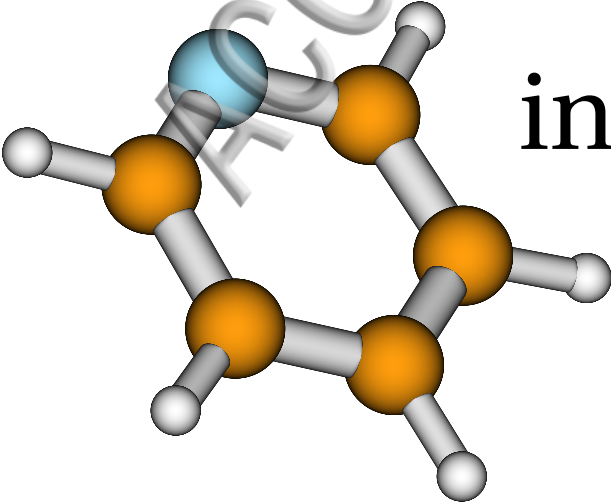
MOLDEN



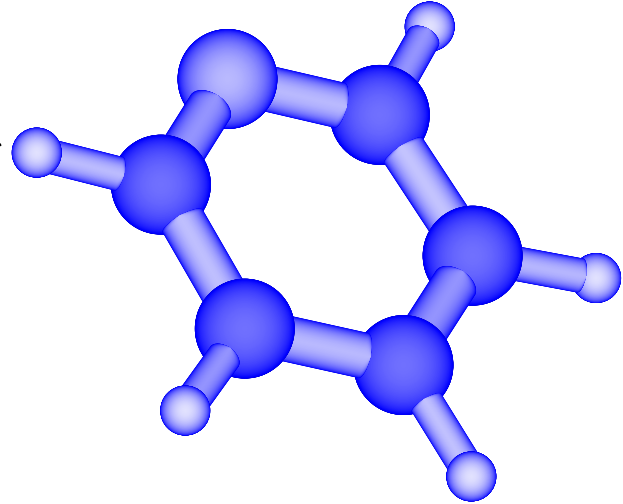
total effect

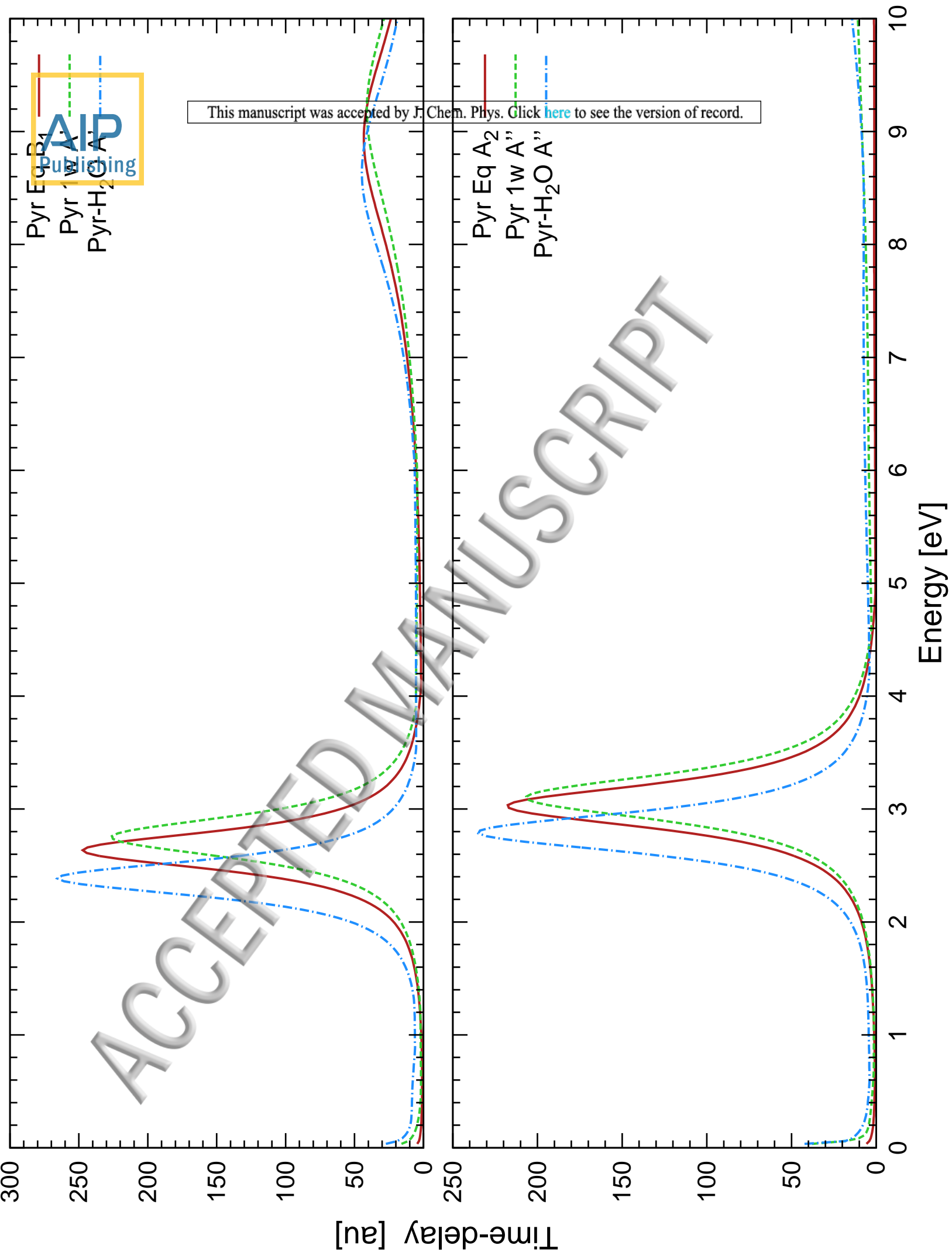


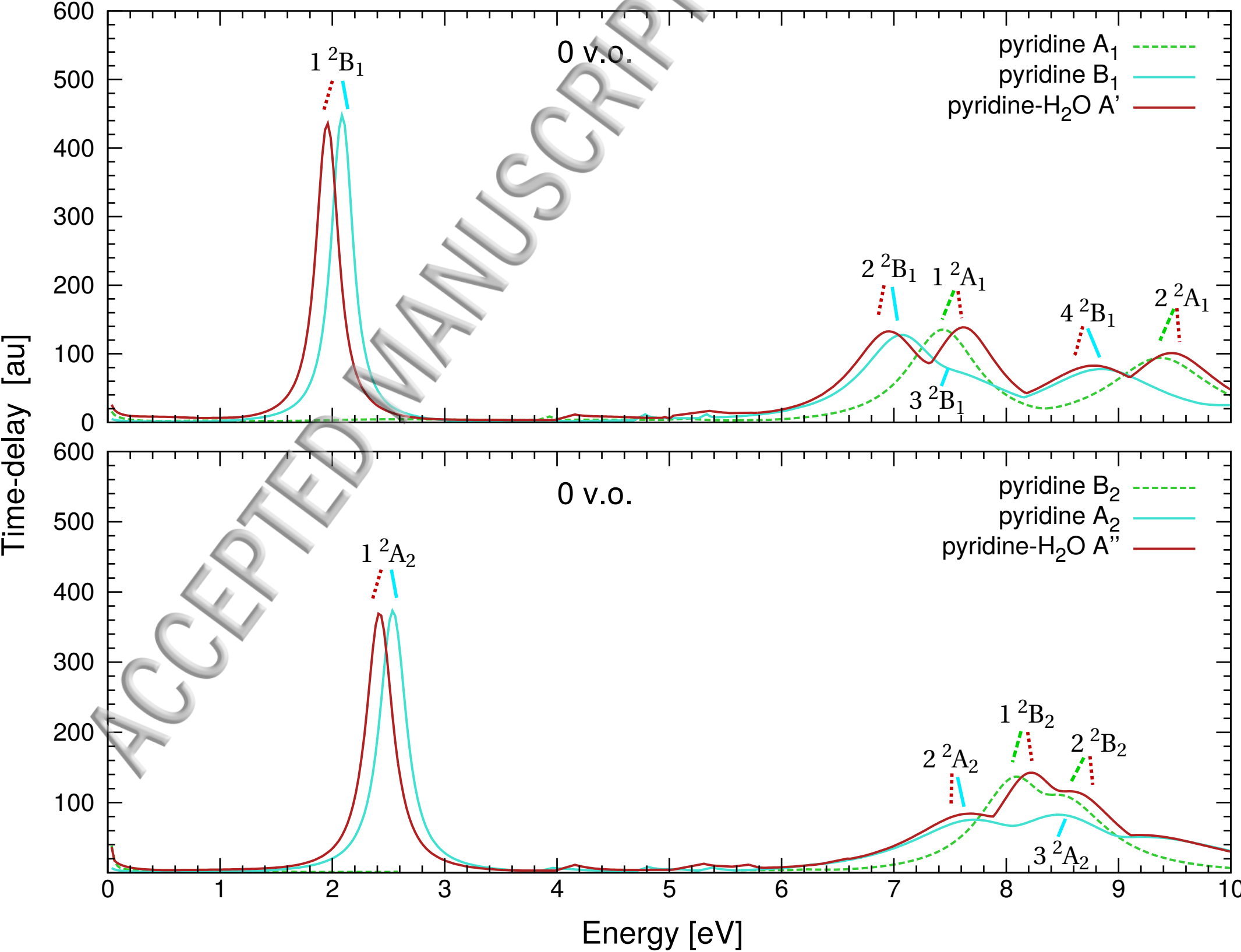


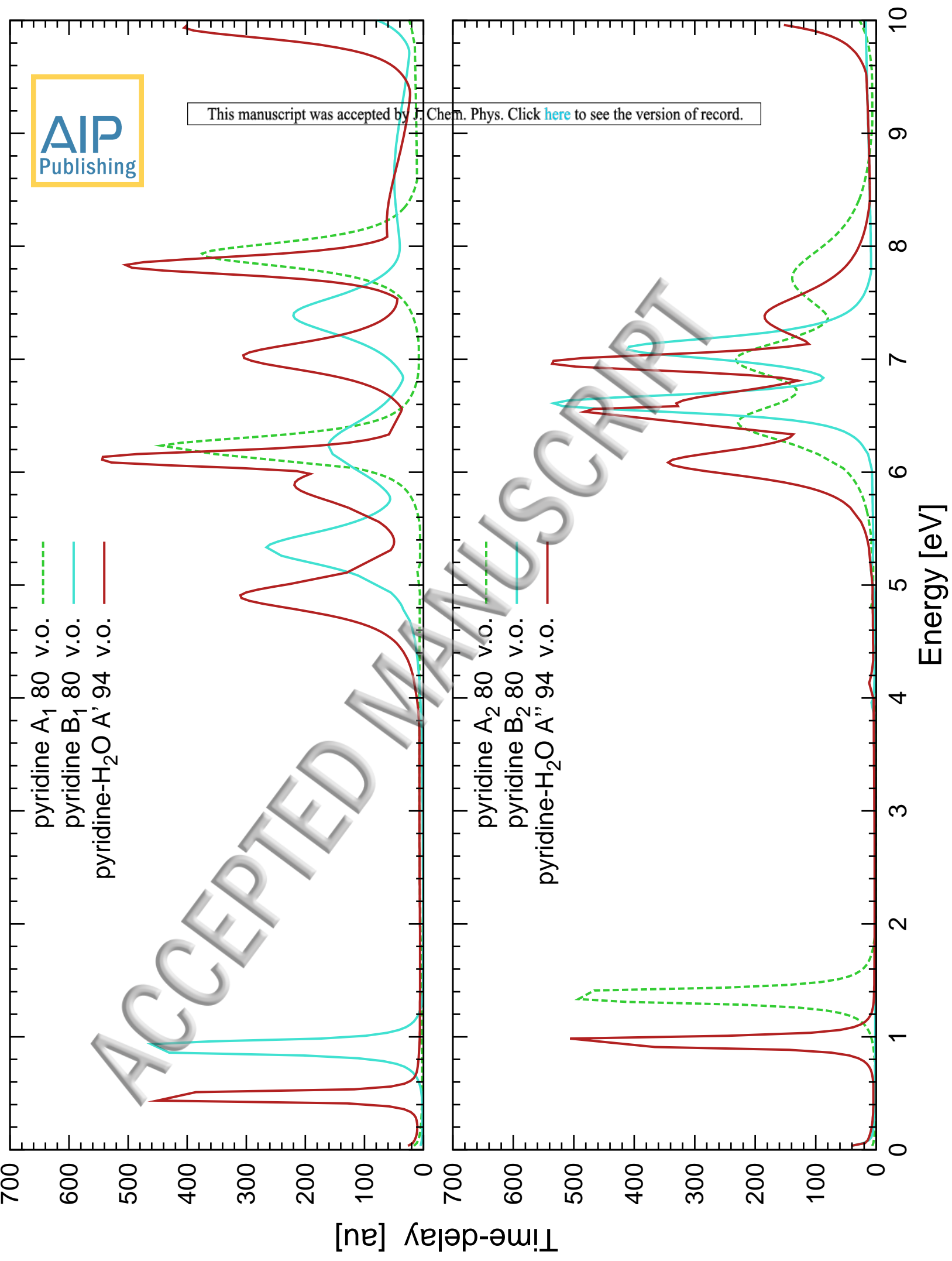


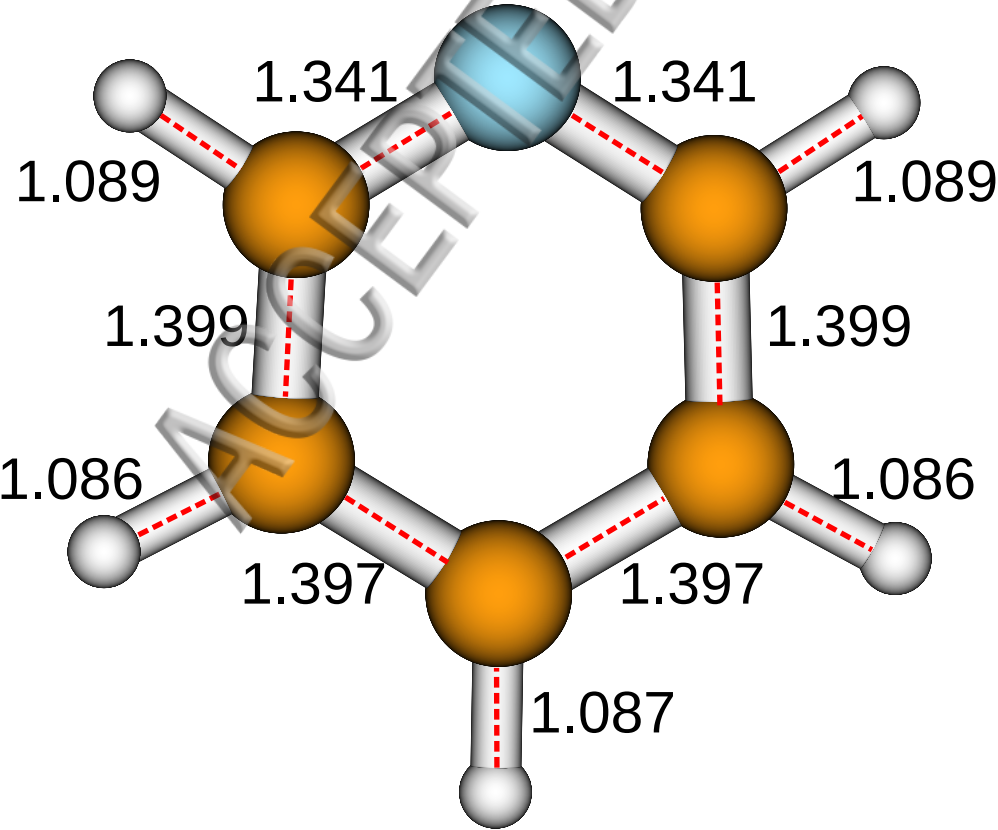
indirect effect

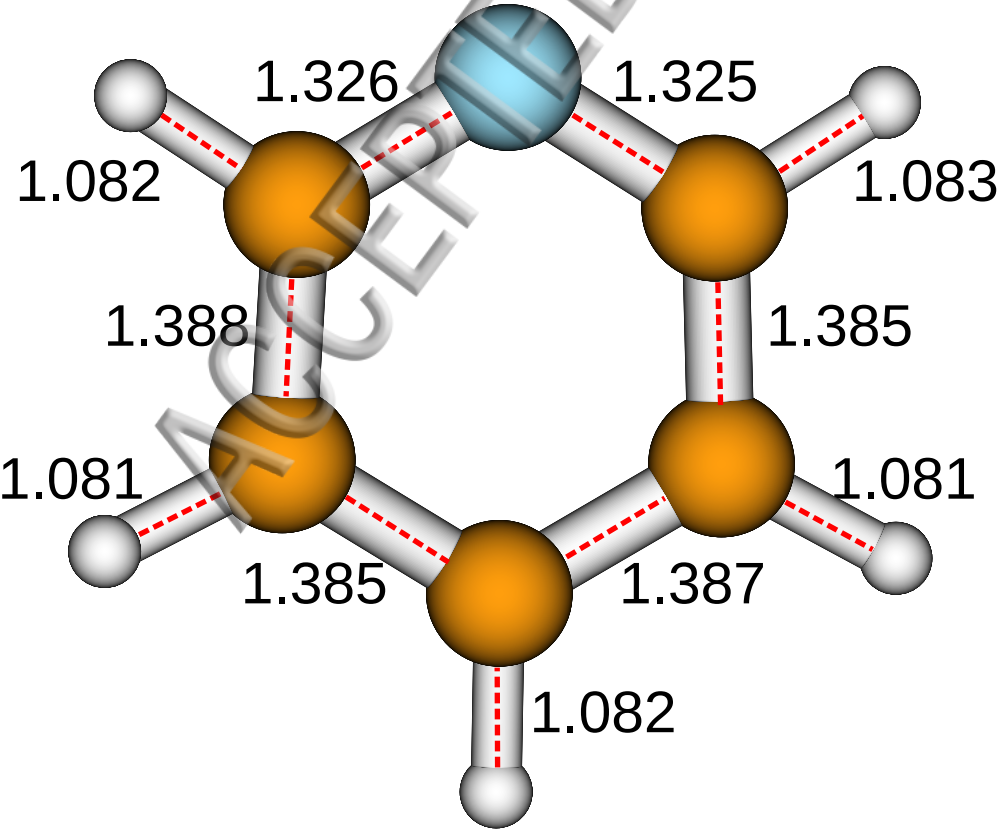


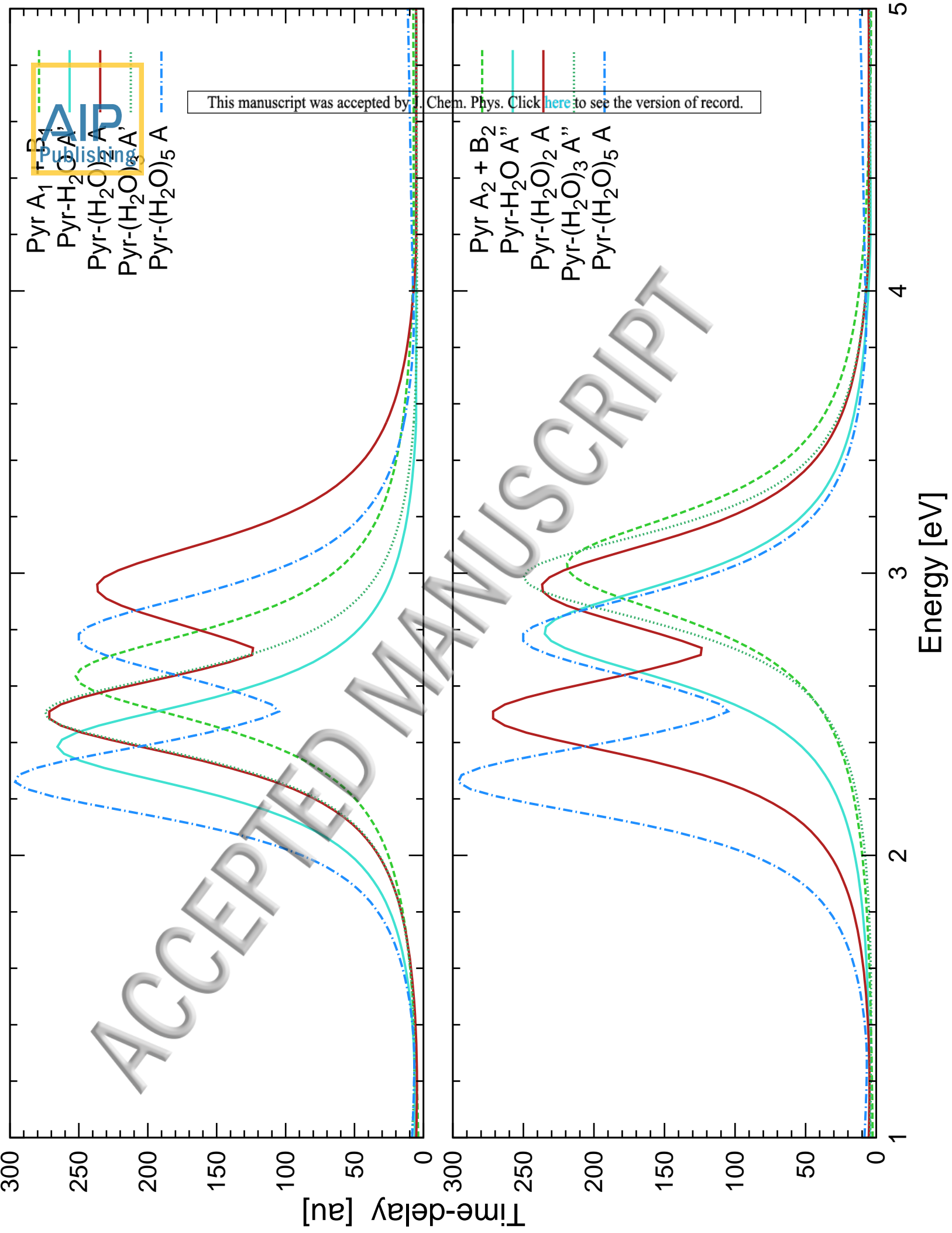


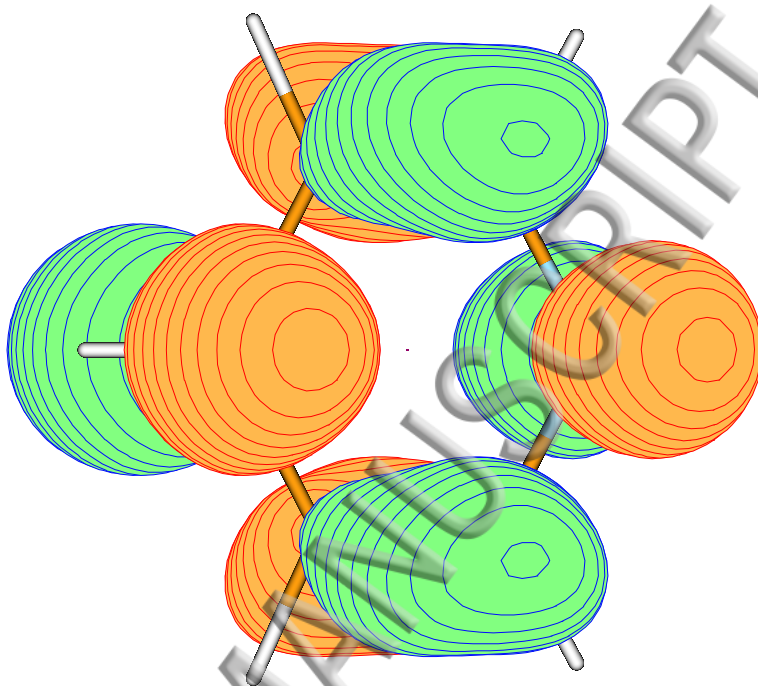










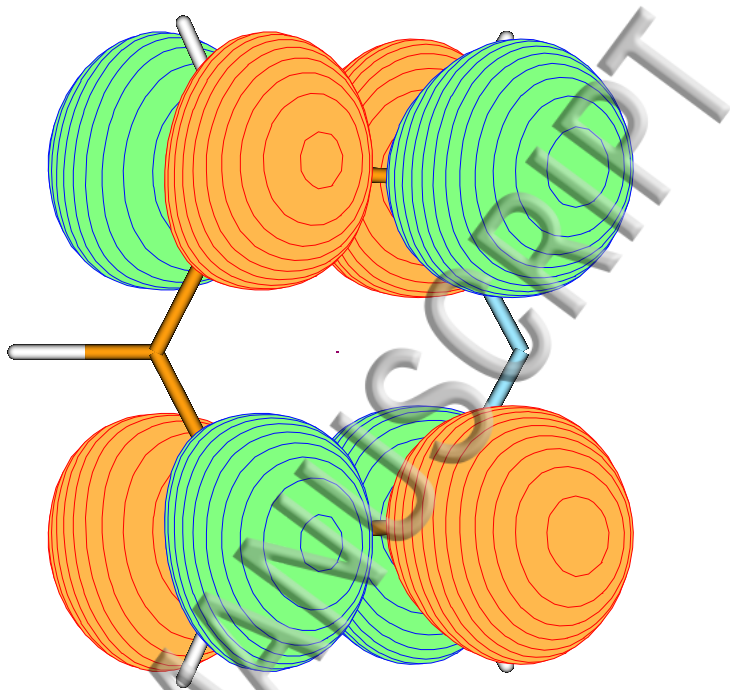


MOLDEN

defaults used

Edge = 11.24 Space = 0.0500 Psi = 22

ACCEPTED MANUSCRIPT



defaults used

Edge = 11.24 Space = 0.0500 Psi = 23

MOLDEN

ACCEPTED MANUSCRIPT